Programmable Drug Control of Receptor Valency Modulates the Potency of Cell Therapeutics

Paul B. Finn[1,2,#], Michael Chavez[1,#], Xinyi Chen[1], Haifeng Wang[1], Draven A. Rane[1], Jitendra Gurjar[2,4], Lei S. Qi[1,2,3,*]

[1]Department of Bioengineering, Stanford University, Stanford, CA, USA
[2]Sarafan ChEM-H, Stanford University, Stanford, CA, USA
[3]Chan Zuckerberg Biohub, San Francisco, CA, USA
[4]Current Address: Novartis Institutes for BioMedical Research, San Diego, CA, USA
[#]Equal contribution
*Corresponding to: stanley.qi@stanford.edu (L.S.Q)

ABSTRACT

An increasing number of preclinical and clinical studies are exploring the use of receptor-engineered cells that can respond to disease states for the treatment of cancer, infectious disease, autoimmunity, and regeneration. However, receptor-based cell therapies, including chimeric antigen receptor (CAR), face many critical issues including target recognition escape, adverse side effects, and lack of *in vivo* control. Drug-controllable receptors offer a promising solution to overcome these issues through precise *in vivo* tuning of cells via enhanced sensing and therapeutic efficacy. Here we develop a novel class of modular and tunable receptors, termed valency-controlled receptors (VCRs), which can leverage customized small molecules to mediate cell signaling strength via controlled spatial clustering. We first develop DNA origami activated VCRs to demonstrate that receptor valency is a core mechanism that modulates immune cell activation. We design a series of customized valency-control ligands (VCLs) by transforming small molecule drugs into a multivalency format and modularly fusing VCR onto the CAR architecture. We demonstrate that VCL induction allows enhanced target sensitivity of engineered cells. Using medicinal chemistry, we develop programmable bioavailable VCL drugs to demonstrate that the VCR system enables drug-induced highly potent responses towards low antigen cancers *in vitro* and *in vivo*. Valency controlled receptors and customizable drug ligands provide a new synthetic biology platform to precisely tune engineered cell therapeutic potency, which can address existing safety and efficacy barriers in cell therapy.

INTRODUCTION

Cells make decisions by integrating a multitude of stimulatory and inhibitory signals from the extracellular space via membrane-bound receptors (*1*, *2*). Tipping the balance of these signals creates an opportunity for developing safe and efficacious cell therapy with controllable therapeutic functions (*3*). The design of synthetic receptors to enable user-defined manipulation of phenotypes has become the backbone of cell engineering and therapies (*4*). As receptor-engineered cells offer a promising living drug for treating cancer, infectious disease, autoimmunity, and regeneration, there is an urgent need for programmable tuning of cell activity *in vivo* to modulate safety and realize the true therapeutic potential of engineered cell (*5*).

One of the best studied synthetic receptors is the chimeric antigen receptor (CAR), which are single chain transmembrane molecules that link TCR-like signaling to user-defined tumor surface antigens (*6*, *7*). CAR T cell therapies targeting CD19 have seen a major clinical success in treating blood malignancies (*8–11*). Despite successes, many challenges remain that limit the safety and potency of receptor-engineered cells (*12–16*). Tumor antigen density is a major factor that influences the efficacy of CAR T cells (*17–19*). When antigen expression is below a threshold, CARs fail to exert antitumor activities. For example, cancer relapse in B cell acute lymphoblastic leukemia (B-ALL) patients has been linked to a reduction in antigen expression below the activity threshold of CARs, and variable antigen densities of the cancer cell population limit cell therapy efficacy in solid tumors (*14*, *20*, *21*). Tuning the threshold for antigen recognition *in vivo* has emerged as a promising strategy to overcome these limitations (*22*). However, it is important to balance receptor activity for effective cancer cell killing while limiting fatal adverse events such as cytokine release syndrome and neurotoxicity (*23*, *24*). Solutions to address such challenges require developing a novel synthetic biology platform to design CAR molecules that enable modular, tunable, and precise control of cell activity *in vivo* (*25*).

Here, we revisited the receptor design scheme, by looking at natural T cell receptor (TCR) biology. TCR signaling is initiated through weak-to-moderate receptor molecule binding to the antigen peptide-loaded Major Histocompatibility Complex (pMHC) (**Figure 1A**) (*26*). From a biophysical perspective, this binding event induces TCR mechanotransduction, or “vertical” signaling, leading to activation of kinase cascades resulting in T cell cytotoxicity (*27*). While mechanosensation is a principal mechanism of action for signaling, the formation of supramolecular microclusters of TCRs at the immunological synapse, or “horizontal” signaling, can amplify the overall TCR signaling (*28–33*). Spatial microclustering is a potential mechanism for modulating TCR signaling strength, and the degree of clustering (i.e., how many molecules are clustered) hypothetically correlates with T cell potency, which can be harnessed to precisely tune T cell cytotoxicity (*34–37*). In contrast to TCR, current CAR designs adopt a one-dimensional (1D) architecture, incorporating only cell-to-cell vertical signaling upon recognition of the antigen by the fused single-chain variable fragment (scFv) (*38*). This design does not fully recapitulate the TCR signaling process, which likely leads to weak T cell cytotoxic responses when recognizing low antigen tumors (*39–41*). To date, little has been done to systematically explore whether precisely controlling the extent of ‘horizontal’ receptor clustering could allow precisely modulating T cell signaling and enhancing cytotoxic activity (*42–44*).

Inspired by the horizontal clustering of TCRs, we develop a new class of tunable receptors utilizing customized small molecules to mediate spatial clustering (**Figure 1B**). By incorporating a multivalent drug binding domain into the extracellular region of receptor, we create a modular architecture termed Valency Controlled Receptor (VCR) that enables drug-inducible receptor clustering. We hypothesize that integrating another dimension of VCR-enabled ‘horizontal’ signaling into CAR-enabled ‘vertical’ signaling (called 2D VCR) would allow for tunable control of potency and spatiotemporal activity of T cells. Upon binding to its multivalent drug, termed valency control ligand (VCL), we can conditionally induce VCR cluster formation that enhances T cell signaling (**Figure 1B**). The 2D VCR system induces vertical signaling upon recognition of the tumor antigen and can be precisely tuned through horizontal signaling. Thus, the VCR platform provides a new mechanism for tuning cell therapy by simply controlling receptor valency via customizable drugs.

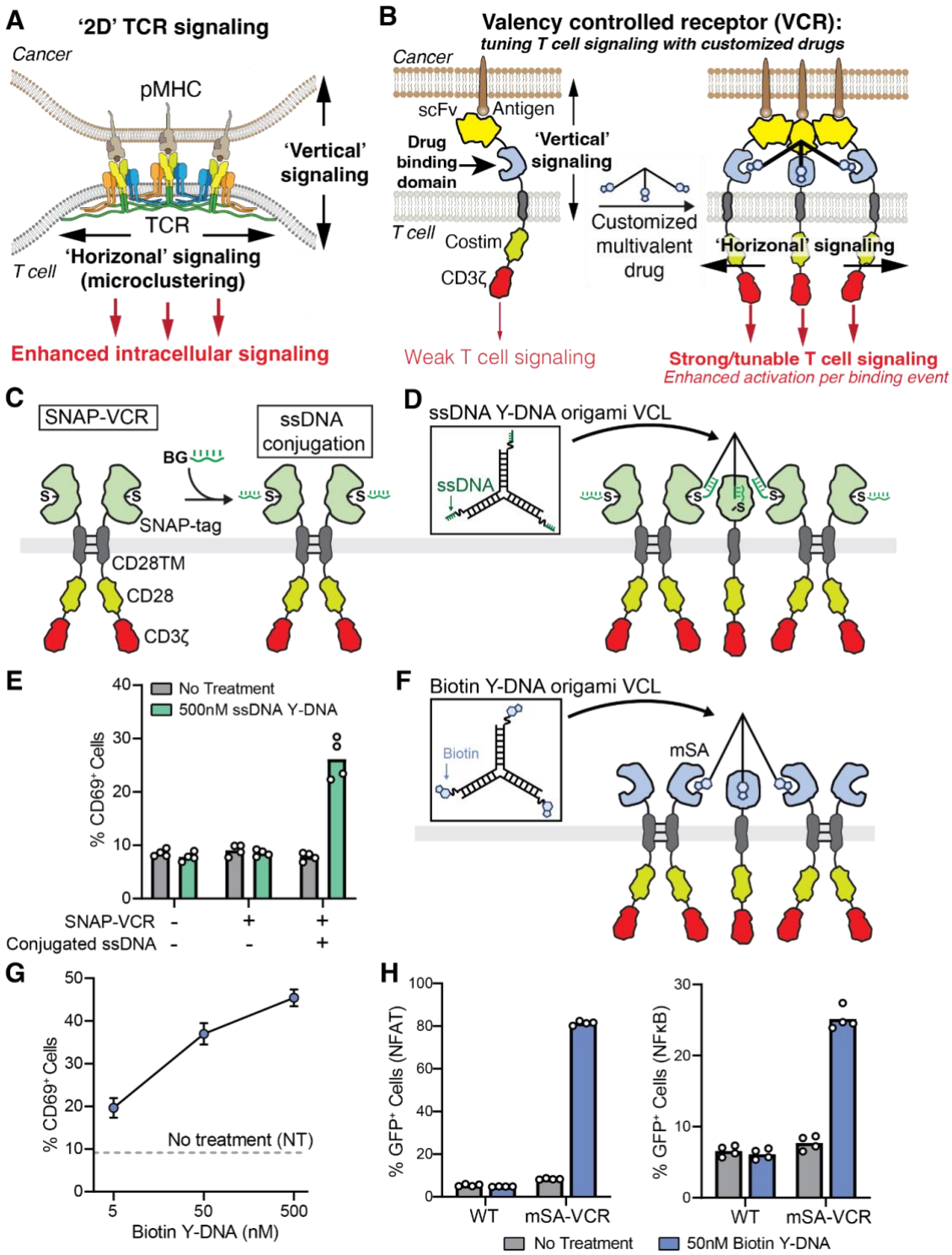

Figure 1: Valency-controlled receptor (VCR) allows drug-inducible immune cell signaling. A) TCR signaling utilizes both 'vertical' signaling (binding between TCR extracellular domain and pMHC) and 'horizontal' signaling (microclustering), which are important for the high potency of T cell signaling. **B)** Schematic of a valency-controlled receptor (VCR) that is built upon a 1D-signaling chimeric antigen receptor (CAR) molecule, by incorporating a multivalent drug binding domain into the extracellular hinge region to enable drug-mediated T cell activation. Dosing with a multivalent drug induces clustering of VCRs to greatly enhance T cell signaling upon antigen binding by combining vertical and horizontal signaling. **C)** Development of a DNA origami ligand-inducible VCR, SNAP-VCR, which contains an extracellular SNAP-tag protein, a CD28 transmembrane domain (CD28TM), a CD28 cytoplasmic domain, and a CD3ζ cytoplasmic domain. SNAP-VCRs are further conjugated with a benzyl guanidine (BG) modified single-stranded DNA (ssDNA) oligo. **D)** The DNA origami scaffold is utilized to create a trivalent ssDNA ligand (ssDNA Y-DNA) that induces clustering of the ssDNA-conjugated SNAP-VCR. **E)** SNAP-VCR induces Jurkat T cell activation when both the ssDNA-conjugated SNAP-VCR receptor and the ssDNA Y-DNA origami ligand (500 nM) are present. **F)** The same Y-DNA origami scaffold is used to generate a trivalent biotin structure (biotin Y-DNA) that interacts with VCR containing an extracellular monomeric streptavidin (mSA). **G)** mSA-VCR Jurkat cells exhibit dose-dependent activation upon addition of the trivalent biotin Y-DNA multivalent ligand. **H)** The mSA-VCR induces NFAT (left) and NFκB signaling (right) in NFAT-GFP Jurkat reporter cells and NFκB-GFP Jurkat report cells, respectively, in the presence of trivalent biotin Y-DNA ligand.

RESULTS

Developing a drug-inducible valency-controlled receptor (VCR)

Developing a drug-inducible VCR system requires engineering of both the drug molecule and receptor. In addition to the drug binding affinity, the proximity between clustered receptors, receptor valency, and cluster dynamics are important parameters that control the receptor signaling response. However, unlike DNA or protein engineering, medicinal chemistry can be a slow and laborious process, limiting our ability to rapidly explore a large space of parameters in parallel. To overcome this limitation, we first developed a flexible, facile, and high-throughput platform to identify both the drug molecule and receptor architecture in parallel.

To establish the VCL-VCR platform, we first adopted a DNA-based receptor design that consists of a single stranded DNA (ssDNA) covalently conjugated via benzyl guanidine (BG) to an extracellular SNAP-tag protein (**Figure 1C**) (*36*). The SNAP-tag, a self-labeling protein tag that can be covalently tagged with a ligand, was fused to intracellular signaling domains (CD28 and CD3ζ) and connected by a IgG4 hinge and CD28 transmembrane domain. This SNAP-VCR (without scFv) can interact with a ssDNA ligand that is complementary to its conjugated ssDNA, and their interaction can be programmed using Watson-Crick base pairing. To induce a higher valency, DNA origami was leveraged to present multiple ssDNA strands by creating a rigid Y-shape structure (valency = 3) that is decorated at the distal ends with ssDNA complementary to the DNA-conjugated SNAP-VCR (**Figure 1D**). Together, this system enables rapid and facile identification of clustering dynamics without sophisticated medicinal chemistry. Expressing the SNAP-VCR in a Jurkat T lymphocyte cell line (JRTE6-1) demonstrated that clustering of VCRs can induce low level T cell activation when the binding domain (SNAP-tag conjugated with ssDNA) and the multivalent ligand (ssDNA Y-DNA origami) were present (**Figure 1E**).

We next sought to develop a more translatable system for using DNA origami to present small molecule moieties. To do this we swapped the SNAP-tag domain for a monomeric streptavidin (mSA) domain (*45*) on the VCR and decorated the Y-DNA origami with covalently attached vitamin B7 (biotin) instead of ssDNA (**Figure 1F**). Our results showed that Jurkat cells expressing the mSA-VCR were activated by treatment with the biotin Y-DNA origami (valency=3) in a dose-dependent manner (**Figure 1G**). Interestingly, clustering of CD28 and CD3ζ without antigen-scFv binding was sufficient to induce both NFAT and NFκB signaling in Jurkat reporter cell lines (**Figure 1H**).

Leveraging DNA origami to characterize multivalent ligand designs for controlling VCR activity

We next utilized the rapid, facile, and inexpensive nature of DNA origami scaffolds to understand how drug design affected VCR-mediated T cell signaling. We asked which other small molecules could induce VCR activity by conjugating a candidate molecule to the Y-DNA origami and engineering a VCR containing the small molecule-binding protein domain. To do this, we swapped mSA-VCR with a fluorescein isothiocyanate (FITC)-binding single-chain variable fragment (scFv), FITC-binding anticalin (FluA), or a human bromodomain-containing protein 4 (BRD4) domain. Correspondingly, we conjugated the Y-DNA origami scaffold with FITC or JQ1 (**Figure 2A**). Our data showed that all designs induced T cell activation in the presence of the trivalent Y-DNA drug ligand and some ligand-VCR pairs induced stronger activation than others. This demonstrates that VCRs can be controlled by different drugs in the multivalent format.

To determine how receptor valency and therefore number of receptors in a cluster affected T cell activation we leveraged the programmability of DNA origami to control the number of ligand moieties available to bind VCRs. We synthesized a library of Y-DNA scaffolds decorated with increasing numbers of biotin molecules (valency = 0~3). Induction of mSA-VCR Jurkat cells by these ligands with different valency showed that higher valency led to increased T cell potency (**Figure 2B**). We next asked how proximity of drug-bound VCRs altered T cell activation. To do this, we increased the arm length of the Y-DNA scaffold by increasing the number of nucleotides from 24 basepairs (bp) to 36 bp. Interestingly, treatment with the shorter scaffold resulted in increased T activation (**Figure 2C**),

indicating that increasing VCR proximity in the cluster led to more effective signaling. This proximity effect was also observed when examining activation-mediated IL-2 production (**Figure 2C**).

To characterize how the ligand valency affects receptor activity, we further probed valency parameters using different DNA origami shapes, including I-DNA (valency = 2), Y-DNA (valency = 3), and X-DNA (valency = 4), all of which were conjugated with biotin (**Figure 2D**). Across three orders of ligand concentration, Y- and X-DNA generated comparable T cell activation and were both superior to I-DNA, which was also observed in a Jurkat NFAT-GFP reporter cell line (**Figure 2E-F**). We next asked if these design principles were also true in primary human T cells. In two different donors' T cells expressing mSA-VCR, both Y- and X-DNA outperformed I-DNA (**Figure 2G**). These experiments indicated that VCL designs should have a valency greater than 2. Furthermore, VCR design rules that are developed in cell lines are translatable to primary human cells.

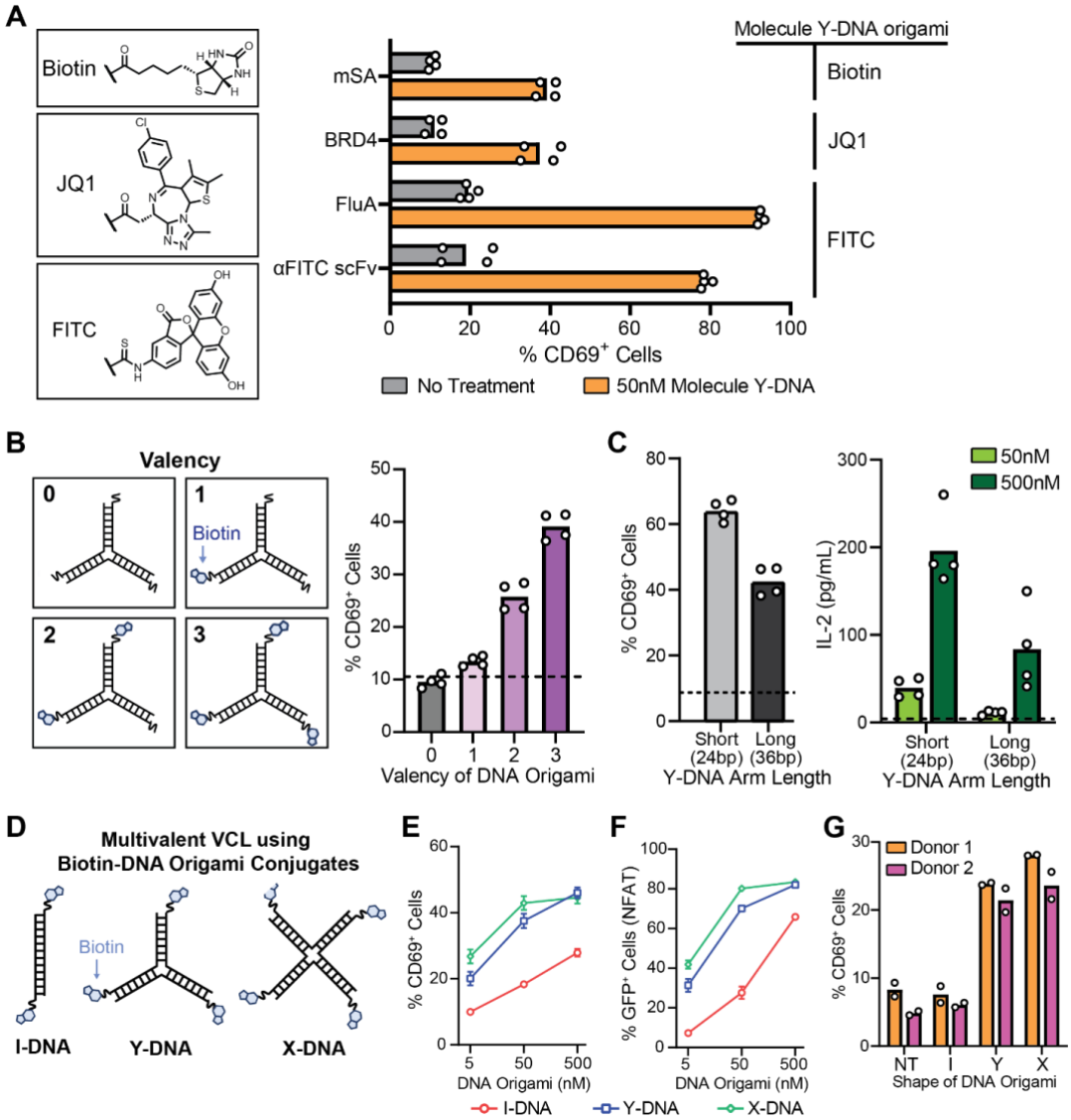

Figure 2: DNA origami enables characterization of VCR-ligand interaction for T cell activation. A) The Y-DNA structure origami was leveraged to create trivalent JQ1 and FITC to induce T cell activation in Jurkat cells for VCRs containing an extracellular BRD4 (with JQ1 Y-DNA), an FluA anticalin (with FITC Y-DNA), and a FITC scFv (with FITC Y-DNA). In the presence of cognate ligand, we observed activation of T cells measured by %CD69$^+$ population. **B)** DNA origami can be programmed to create Y-DNA with increasing biotin valency and probe its effects on VCR-mediated T cell activation. Increased valency leads to a higher percentage of CD69$^+$ activated T cells. **C)** Closer proximity between biotins in the Y-DNA structure (20 bp vs 36 bp for the Y-DNA scaffold arm) increases T cell activation, as quantified by percentage of CD69$^+$ population (*left*) or IL-2 production (*right*). **D)** DNA origami is programmed to create I-DNA (bivalent), Y-DNA (trivalent), or X-DNA (tetravalent) scaffolds for biotin. **E-F)** Jurkat cells expressing mSA-VCR are dosed with I-DNA, Y-DNA, or X-DNA origami. T cell activation is comparable for using X- and Y-DNA and higher than using I-DNA as measured by %CD69$^+$ cells and NFAT signaling. **G)** Activation of two donors of primary human T cells are observed using X- and Y-DNA but not for I-DNA.

Development of programmable multivalent small molecule drugs to control VCRs

We next sought to translate the multivalent DNA origami ligands into drug molecules. To convert a customized drug into a multivalent format that recapitulates the DNA origami design, we utilized dendrimer scaffold chemistry. While both the 3- and 4-valency designs performed similarly in our DNA system, the X design is more accessible via commercially available chemical scaffolds. We used peptide coupling chemistry to covalently conjugate biotin to a generation 0 PAMAM dendrimer and generated a lead multivalent small molecule, termed 4° Bio VCL (**Figure 3A**). We confirmed that 4° Bio VCL cab effectively activate the NFAT pathway in mSA-VCR Jurkat reporter cells (**Figure 3B**).

Clinically relevant CAR designs contain other costimulatory signaling domains in addition to the CD28 domain. To determine if the VCR system could activate receptors containing a 4-1BB costimulatory domain, we generated and tested a VCR-BBζ receptor in both NFAT and NFκB reporter Jurkat cells. We observed that while VCR-28ζ induced strong NFAT signaling in the presence of 4° Bio VCL drug (**Figure 3C**), the VCR-BBζ induced strong NFκB signaling (**Figure 3D**). Additionally, VCRs without a costimulatory domain can also activate NFAT signaling but to a much lesser extent.

To extend the utility of the VCR platform, we generated VCRs containing only the 4-1BB signaling domain. The 4° Bio VCL-mediated clustering of VCR-BB effectively induced NFκB signaling and synergized with antibody-mediated CD3 signaling (**Figure 3E**). This indicates the potential for the VCR platform to control costimulatory signaling for applications beyond CAR T cells, for example, in combination with TCR T cell therapies.

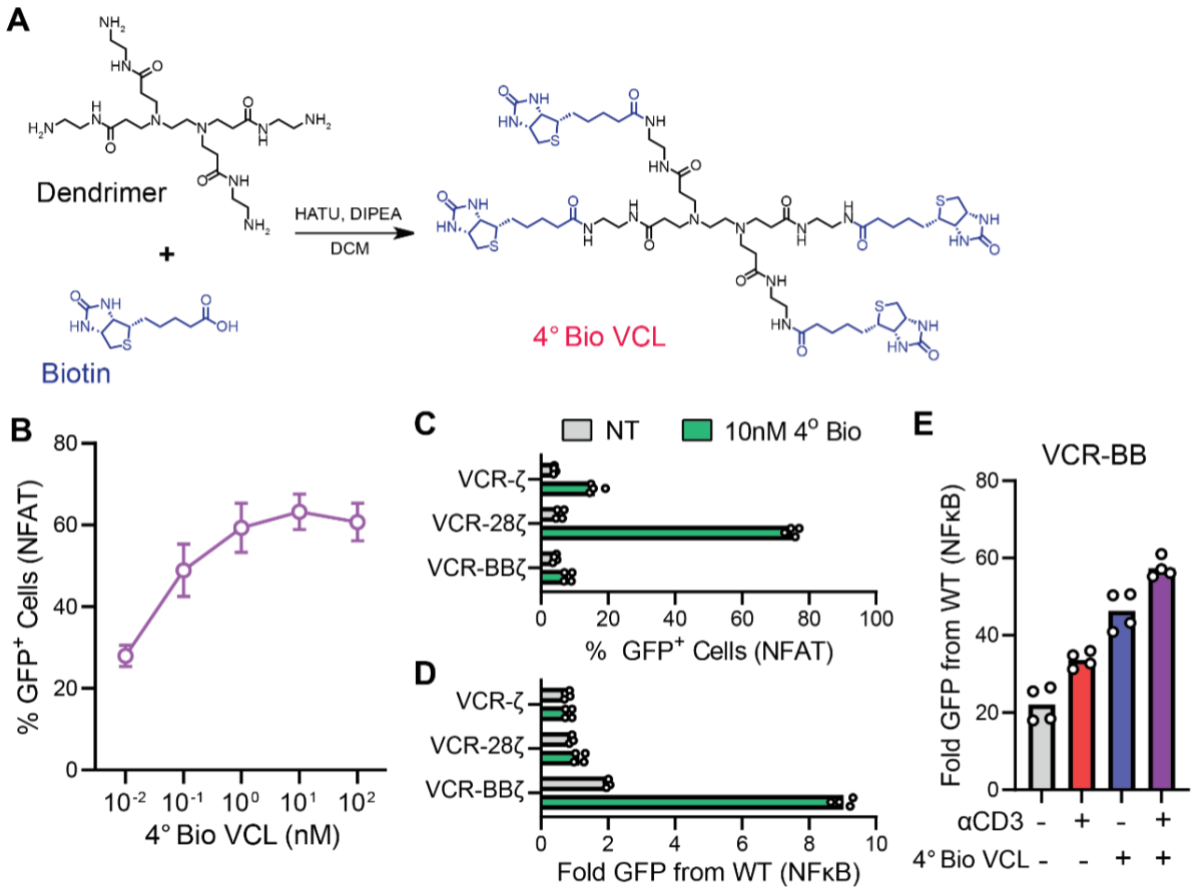

Figure 3: Development of multivalent small molecule ligands to modulate VCR T cell activation. A) Using a generation 0 PAMAM dendrimer scaffold, a tetravalent biotin compound was synthesized to create a small molecule version of the biotin X-DNA (4° Bio). **B)** 4° Bio VCL induced NFAT signaling in VCR engineered NFAT-GFP Jurkat reporter cell lines. **C-D)** VCRs containing a CD28 costimulatory domain and dosed with 4° Bio activates NFAT signaling, while VCRs containing a 4-1BB costimulatory domain and dosed with 4° Bio activates NFκB signaling.

Higher valency-mediated super-clustering of VCR amplifies T cell signaling

The IgG4 hinge and CD28 transmembrane domains used in the VCR system contain cysteine residues and hydrophobic residues with the ability to form S-S bonds and π-π stacking interactions, respectively. These interactions lead to the formation of dimeric VCRs on the surface of the cell creating the possibility that the VCL is not simply creating small clusters of VCRs based on ligand valency (clusters of four VCRs when treated with 4° Bio VCL), but instead is inducing "daisy-chaining" of many VCRs into larger clusters (**Figure 4A**).

To probe this hypothesis, we expressed an mSA-VCR fused to a fluorescent protein (mSA-VCR-GFP) in HEK293T cells and performed confocal microscopy to visualize the formation of receptor clusters upon treatment with 4° Bio VCL. After 30 minutes of VCL treatment, diffused GFP membrane signals formed large puncta at the cell surface, indicating the formation of large receptor clusters (**Figure 4B**).

To further investigate whether this potential super-clustering affected T cell signaling, we engineered a monomeric version of mSA-VCR by mutating the cysteine residues in the hinge domain and the transmembrane domain residues responsible for hydrophobic interactions. When treated with 4° Bio VCL we observed increased NFAT activity by the dimeric VCR compared to the monomeric VCR (**Figure 4C**). However, in the presence of a bivalent biotin (2° Bio VCL), the monomeric VCR lost all signaling capacity while the dimeric VCR was still able to respond (**Figure 4D**). This suggests that the cluster size of monomeric VCRs is dictated by VCL valency, but this is not the case for dimeric VCRs. Taking data together, we conclude that VCR architectures containing cysteine residues and hydrophobic residues can form large super-clusters via daisy chaining, leading to enhanced T cell signaling akin to TCR-based clustering.

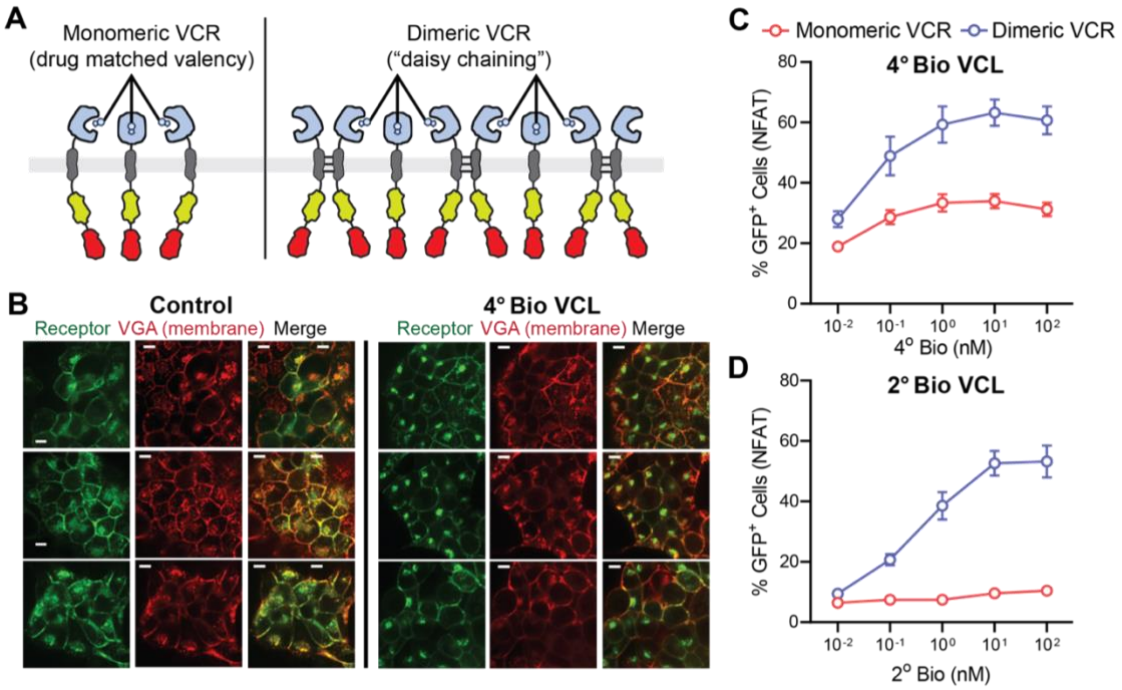

Figure 4: Higher valency-mediated super-clustering of VCR amplifies T cell signaling. A) The hinge and transmembrane domains are mutated to create a monomeric version of VCR by disrupting C-C disulfide bonds and transmembrane interactions. Monomeric VCRs presumably generate receptor clusters that are dictated by the valency of the drug. The original dimeric VCRs can create larger clusters through drug-mediated daisy chaining of multiple clusters. **B)** Confocal microscopy images of HEK293T cells expressing mSA-VCR fused to GFP with and without tetravalent 4° Bio drug for 30 minutes. Green, receptor; red, cell membrane. **C-D)** Using the tetravalent 4° Bio VCL, the monomeric VCR performed worse than dimeric VCR. However, using a bivalent ligand, the monomeric VCR fails to signal, indicating that the drug can induce VCR super-clustering via daisy chaining.

Development of 2D VCR by incorporating VCR into CAR designs for drug-inducible T cell signaling

We next incorporated a CD19 scFv by fusing FMC63 to the N-terminal end of mSA-VCR (FMC-mSA-VCR) to develop a 2D VCR system. To test whether VCR-mediated signaling synergizes with tumor antigen-induced T cell activation signaling, we co-cultured VCR-19BBζ Jurkat cells with CD19$^+$ Nalm6

leukemia cells with and without 4º Bio VCL (**Figure 5A**). We observed that VCR-mediated clustering synergized with CD19 antigen-induced NFAT activity, resulting in a two-fold enhancement of T cell activation in the presence of VCL. This enhancement was also observed when targeting clinically relevant solid tumor antigens, including human epidermal growth factor receptor 2 (HER2). When we co-cultured VCR-HER2BBζ with HER2$^+$ Nalm6 cells, we observed similar VCR-mediated enhancement of T cell activity, which demonstrates the modularity of the system relative to tumor antigens (**Figure 5B**).

Using live cell microscopy, we tracked GFP-expressing CD19+ Nalm6 cells co-cultured with human primary T cells engineered with VCR-19BBζ and quantified the abundance of tumor GFP signal (integrated intensity) with and without 4º Bio VCL for every 2 hours over 60 hours (**Figure 5C**). VCL-induced VCR clustering increased the cytotoxicity of VCR-19BBζ T cells, as demonstrated by the tumor GFP signal remaining at 60 hours for using two different donors' T cells (**Figure 5D**). Similarly, we co-cultured VCR-HER2BBζ T cells with a HER2+ 143B osteosarcoma spheroid model. We observed increased killing activity by VCR-HER2BBζ T cells over a 72-hr period when treated with VCL (**Figure 5E**). These data suggest that incorporating drug-mediated horizontal signaling into the CAR signaling domains as a 2D VCR system significantly enhances tumor killing *in vitro*.

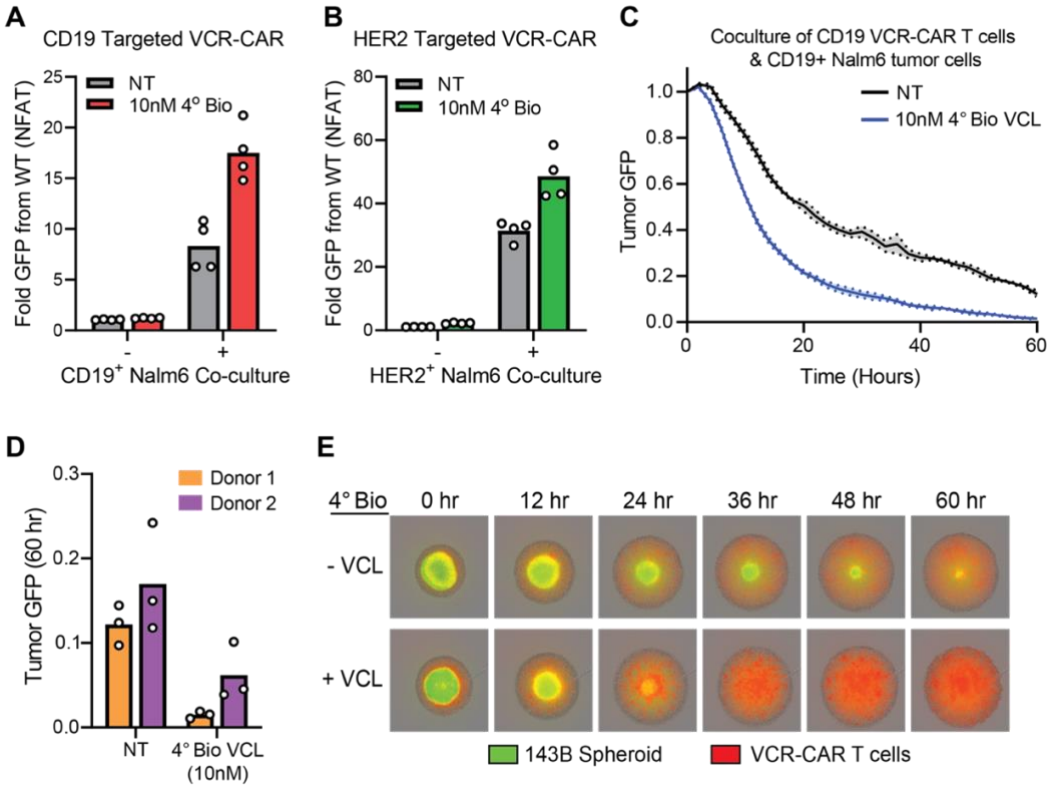

Figure 5: 2D VCR receptors show synergistic antigen-binding activity with VCL-mediated VCR clustering. A) VCR fused to a CD19-targeted scFv (VCR-19BBz) activates NFAT signaling in Jurkat reporter cells in the presence of CD19$^+$ Nalm6 cells and is enhanced by 4º Bio VCL treatment. **B)** HER2 targeted 2D VCR T cells (VCR-HER2BBz) activate NFAT signaling in the presence of HER$^+$ Nalm6 cells and are enhanced by treatment with 4º Bio VCL. **C)** Real-time live cell microscopy imaging of the co-culture of VCR-19BBz-engineered primary human T cells with CD19$^+$ Nalm6 cells (1:1 E:T ratio) showed enhanced tumor killing, by comparing cultures treated with 4º Bio VCL (blue) or no treatment (black). **D)** Final tumor cell densities (at 60 hours) were consistently reduced with VCR-19BBz-engineered primary T cells across different donors. **E)** VCR-HER2BBz-engineered primary T cells (red) exhibited greatly improved cytotoxicity against HER2+ 143B bone osteosarcoma spheroids (green).

Lead VCL drug optimization enables 2D VCR-mediated cytotoxicity in vivo

To translate the VCL-VCR concept into a therapy, we next designed a series of small molecules (PBF001~PBF004) by varying the linker and measured their half-life *in vivo* (**Figure 6A**). We tested this series of designed VCL drugs and determined the half-life of PBF002 and PBF004 to be approximately 4 hours, while PBF001 and PBF003 were less than 15 minutes. We quantified VCL-induced T cell activation using the *in vitro* VCR-NFAT reporter system. PBF004 performed

significantly better at low concentrations (pM to sub-nM) compared to PBF001 or PBF002 and was chosen for further efficacy testing *in vivo* (**Figure 6B**).

We analyzed plasma concentration of PBF004 after a 10 mg/kg intraperitoneal injection (i.p.) in wildtype mice and confirmed that PBF004 was in the effective range of drug concentration over a 24 h period (**Figure 6C**), which suggested that a drug dosing schedule of 10 mg/kg per day could be sufficient for *in vivo* 2D VCR activation. We next tested VCR-19BBζ T cell activity *in vivo*. We injected $1x10^6$ luciferase-expressing $CD19^+$ Nalm6 cells by tail vein injection into a NOD/SCID mouse and $3x10^6$ 2D VCR-CAR+ T cells intravenously by tail vein 4 days later (**Figure 6D**). Mice were dosed with PBF004 at 10 mg/kg (i.p.) every day for a total of 21 days and tumor burden was measured by bioluminescence imaging (BLI) three times a week. BLI measurements were continued for 14 days after completion of the 21-day VCL treatment for a total of 40 days. This allowed for observation of VCR-19BBζ T cell reversibility when drug treatment is stopped. Mice treated with a combination of VCR-19BBζ T cells and PBF004 had significantly reduced tumor burden compared to mock and VCR-19BBζ T cell without VCL groups (**Figure 6E-F**). Importantly, VCL drug treatment conferred a strong survival benefit (**Figure 6G**).

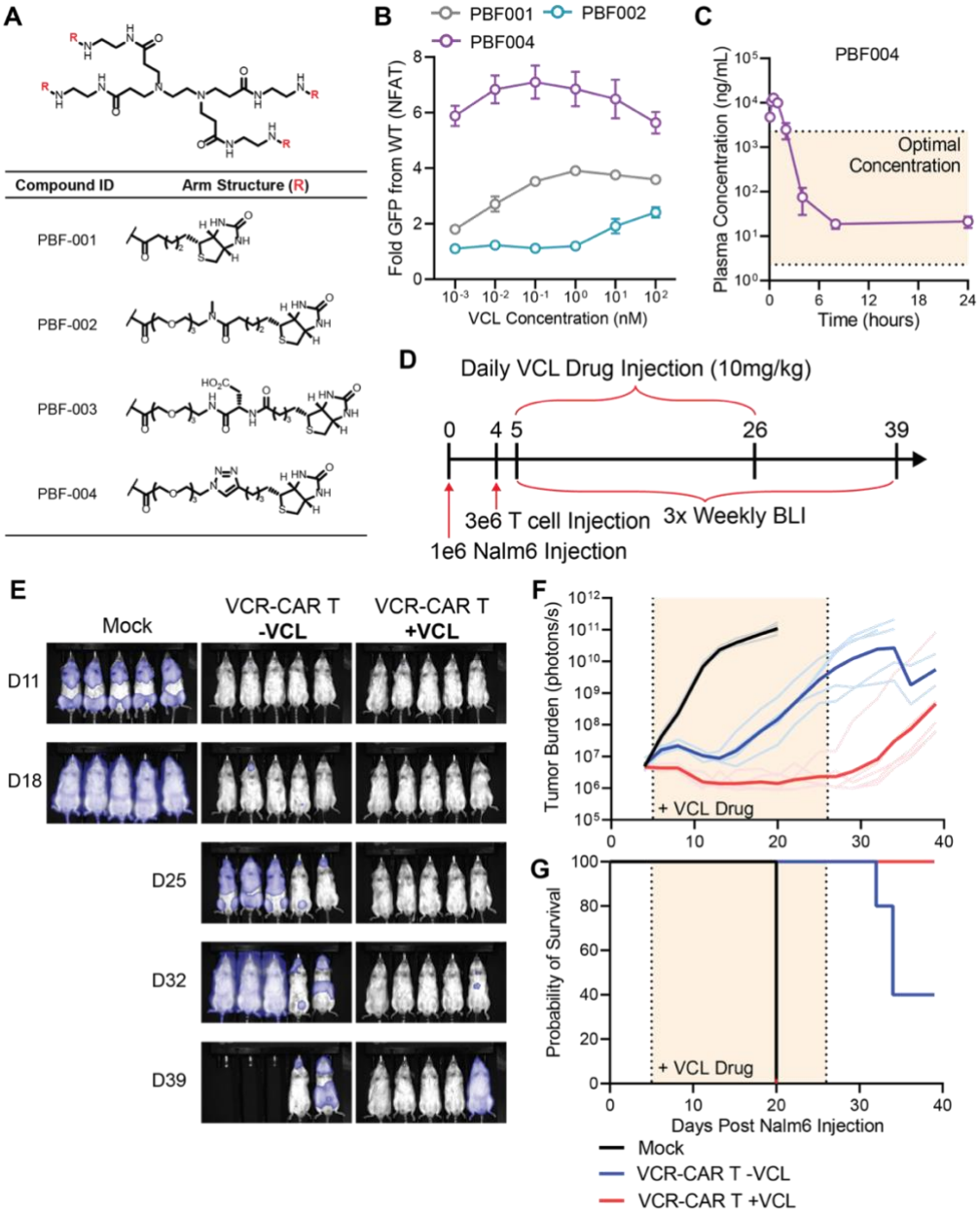

Figure 6: Tetravalent bioavailable VCL drug modulates tumor killing in vivo. A) A series of tetravalent biotin drugs were designed and synthesized with different linkers and conjugated to a generation 0 PAMAM dendrimer to improve bioavailability. **B)** Characterization of PBF001, PBF002, and PBF004 for the activation of mSA-VCR-28z Jurkat reporter cells. **C)** Characterization of PBF004 plasma concentration in the mouse serum over 24 hours. **D)** Schematic overview of

the animal experiment. 1x 10^6 $CD19^+$ Nalm6 cells are i.v. injected into mice and 4 days later, 3 x 10^6 T cells (mock) or 3 x 10^6 VCR-19BBz-engineered T cells are i.v. injected. One group of mice are dosed by i.p. injection with PBF004 daily for 21 days and tumor burden is measured by BLI thrice weekly. **E)** BLI images showing groups of mice injected with mock T cells, VCR-19BBz-engineered T cells without VCL, and VCR-19BBz-engineered T cells with VCL, over time. **F)** Characterization of tumor burden (photon/s) for VCL-dosed mice carrying 2D VCR T cells (red), non-treated mice carrying 2D VCR T cells (blue), and control (black). **G)** Viability curve for VCL-dosed mice carrying 2D VCR T cells (red), non-treated mice carrying 2D VCR T cells (blue), and control (black).

2D VCR sensitizes T cells to low antigen cancers

A common escape mechanism for CD19+ cancers targeted by CAR T cells is decreased surface expression of CD19. Our data showing enhanced cytotoxicity of drug activated 2D VCR T cells toward the HER2+ 143B osteosarcoma model (a low HER2-expressing model) suggested that programmable receptor clustering by our VCR platform could potentially sensitize CAR T cells to low antigen density tumors. To further test this hypothesis, we co-cultured VCR-19BBζ T cells with a recently developed $CD19_{low}$ Nalm6 tumor model (*22*). VCR-19BBζ T cells from different donors with VCL treatment vastly outperformed cells without VCL treatment, suggesting low antigen tumor recognition can be greatly enhanced when inducing higher receptor valency (**Figure 7A**). To determine if 2D VCR T cells can enhance low antigen tumor killing *in vivo*, we generated a $CD19_{low}$ Nalm6 model which has been shown in previous studies to be difficult to control using current CAR designs (*22*). We used the same *in vivo* experimental design shown in **Figure 6D**, with daily PBF004 injection at 10 mg/kg (i.p.) for 21 days and BLI measurement 3 times per week for 40 days. Mice treated with VCR-19BBζ T cells and PBF004 displayed significantly reduced tumor burden compared to the mock and VCR-19BBζ T cells without VCL groups (**Figure 7B-C**). Additionally, mice that were dosed with PBF004 showed a significant survival advantage, while all mice not dosed with PBF004 performed only marginally better than mock and still succumbed to the cancer (**Figure 7D**). Taken together, the data suggests the 2D VCR T cells offers a drug-inducible enhancement of targeting low antigen tumors.

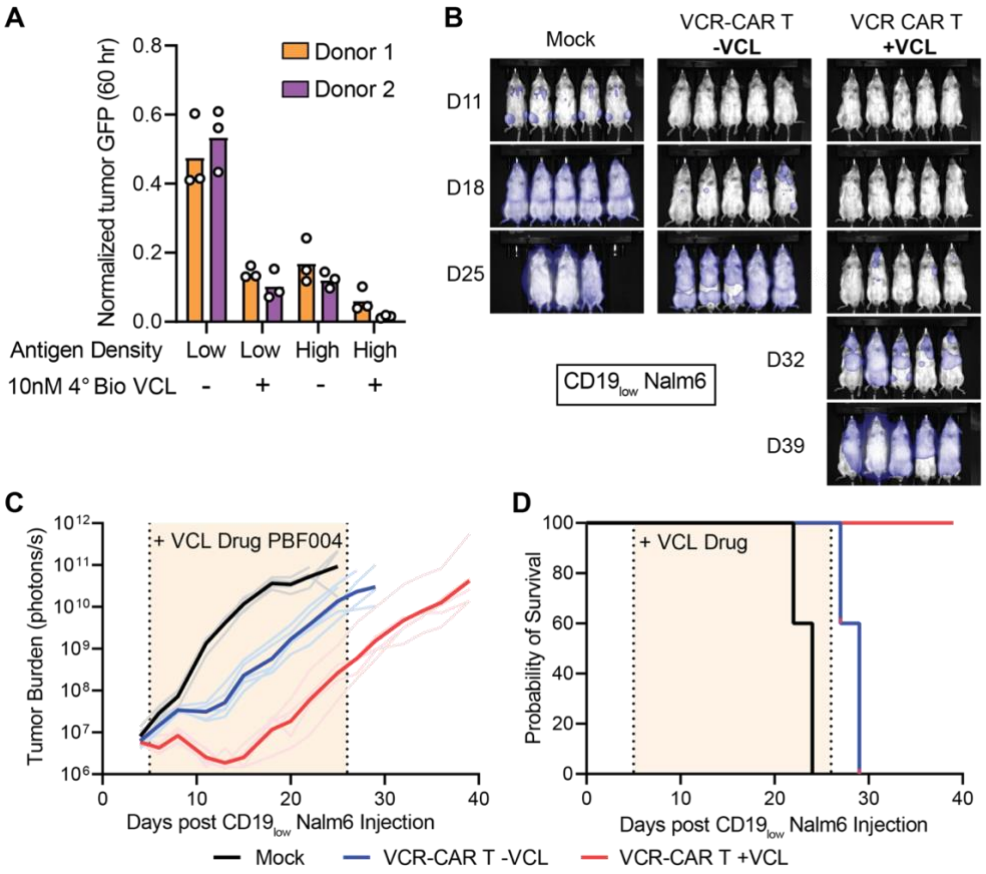

Figure 7: Multivalent drug induces 2D VCR T cells to kill low antigen cancer. A) Characterization of tumor GFP signal using real-time live cell microscopy for two different donors, primary T cells engineered with VCR-19BBz and co-cultured with $CD19_{low}$ or $CD19_{high}$ Nalm6 cells, with and without 10nM 4º Bio VCL. **B)** BLI images showing groups of mice injected with mock T cells, VCR-19BBz-engineered T cells without VCL, and VCR-19BBz-engineered T cells with VCL, over time, all injected with $CD19_{low}$ Nalm6 cells. **C)** Characterization of $CD19_{low}$ Nalm6 tumor burden (photon/s) for VCL-dosed mice

carrying 2D VCR T cells (red), non-treated mice carrying 2D VCR T cells (blue), and control (black). **D)** Viability curve for VCL-dosed mice carrying 2D VCR T cells (red), non-treated mice carrying 2D VCR T cells (blue), and control (black).

DISCUSSION

In this study, we generated a novel valency-controlled receptor platform termed VCR by mimicking the horizontal signaling capabilities of the TCR via a drug-induced valency control mechanism. We utilized DNA origami as a high-throughput and quantitative method to explore parameters that affect drug-receptor interaction. By leveraging the programmability of DNA origami, we developed multiple drug-receptor pairs and characterized both receptor (i.e., cluster size and proximity) and ligand (i.e., valency and concentration) parameters for T cell activation, without the need to perform sophisticated medicinal chemistry. With this knowledge, we designed and synthesized a series of multivalent small molecule drugs that enabled dose-dependent control of VCR T cell activity *in vitro.* We incorporated the identified VCR into the CD19-CAR architecture and demonstrated that addition of a drug molecule could boost VCR T cell cytotoxicity against B cell cancer *in vivo*, resulting is significant control of tumor burden when dosed with drug. We further demonstrated that VCR- CAR T cell activity could be tuned for targeting a low antigen B cell cancer *in vivo*. Treating mice with both 2D VCR T cells and drug provided a significant survival advantage compared to no-drug groups.

For cancer immunotherapy applications, the ability to precisely tune CAR activity *in vivo* during patient treatment using customized drugs has a major impact on clinical outcomes. However, current CAR designs do not allow for this level of *in vivo* control. The VCR platform can be modularly engineered into the CAR architecture to create additional parameter space to enhance and precisely amplify CAR activity *in vivo*. VCR incorporation adds a new dimension of cluster signaling to the CAR architecture. While excessive CAR signaling due to uncontrollable clustering can lead to T cell dysfunction, incorporation of drug-inducible VCR into a CAR provides controllable clustering only in the presence of a paired small molecule drug (*47*, *48*). In addition, other drug-inducible CAR controls could be incorporated with the VCR platform including methods to control receptor expression (e.g., degron-mediated decay and promoter-mediated expression) or safety switches (e.g., SNIP and CRASH-IT) to enhance efficacy and limit toxicities (*49–52*). Furthermore, the VCR platform could be incorporated into SynNotch systems for AND-gating (*53*). While other drug-inducible systems are often designed around a single drug molecule with limited pharmacokinetic properties (e.g., requirements to penetrate the cell membrane), the VCR platform provides a unique system for the rapid identification and programmable design of customized multivalent drugs without the need to enter cells (*54–57*). It is conceivable that many clinically relevant drugs can be converted into a multivalent format to modulate VCR activity *in vivo*, which greatly expands the repertoire of small molecules that can be repurposed for controlling *in vivo* cell therapy. Furthermore, our design of 2D VCR-CAR system has minimal changes (addition of ~1kb) to the current CAR design and is fully compatible with the CAR T manufacture process using a single lentivirus or retrovirus.

By integrating customized small molecule drug control into T cell therapy, the VCR platform enables clinicians to make decisions on the timing and potency of the therapy, thus creating novel avenues for safer and more effective treatments for a myriad of cancers and other diseases. In a future clinical setting using VCR T cells, the drug dosing schedule could be modified as tumor cells undergo reduction of antigen expression. Additionally, dosing schedules could be tested to limit potential side-effects and increase safety by reducing or stopping drug treatment. Moreover, tumor localized drugs (e.g., conjugated to an antibody that binds to tumor antigens) could be explored to ensure T cells are only activated at the site of cancer, reducing the off-target effects often seen in solid tumor CAR T cells (*58*, *59*). As our understanding deepens on how to induce VCR T cells *in vivo*, more complex dosing schedules could be leveraged such as oscillatory regiments that could help overcome T cell dysfunction (*50*, *60*, *61*).

It is possible that the VCR platform can be generalized to other receptor systems beyond CARs. For example, by incorporating VCR into FGFR-mediated signaling, customizable drugs can be used to modulate pluripotency and proliferation of stem cells both *in vitro* and *in vivo*. This would further extend the application of VCR beyond cancer therapy to areas such as stem cell therapy or tissue regeneration. The development of the VCR system expands our synthetic biology arsenal to address

key bottlenecks faced by cell therapies, thus representing a further step forward towards safer and more controllable cell therapies using medicinal chemistry.

ACKNOWLEDGEMENTS

The authors thank all members from Lei Stanley Qi lab for facilitating experiments and discussion. The authors thank Dr. Robbie Majzner for providing the Nalm6 cell lines and useful discussion. The authors thank Nghi Le and Ian Anderson from the Stanford University Protein and Nucleic Acid Facility for DNA origami synthesis. *In vivo* experiments were contracted to the Stanford Transgenic, Knockout and Tumor model Center (TKTC). Chemical synthesis was contracted to WuXi Apptec Limited. The authors thank Nirk E. Quispe Calla, Jasmine Sosa and Hong Zeng from the Stanford Transgenic, Knockout and Tumor model Center (TKTC) for animal experiments. P.B.F acknowledges support by Stanford Maternal & Child Health Research Institute (MCHRI). M.C. acknowledges support by the National Science Foundation Graduate Research Fellowship Program, the ARCS Foundation Scholarship, and the Ruth L. Kirschstein National Research Service Awards for Individual Predoctoral Fellowship (F31AI164936). X.C. acknowledges support by the Stanford Bio-X SIGF Fellowship. L.S.Q. acknowledges support by the Li Ka Shing Foundation, National Science Foundation CAREER award, National Institutes of Health, Stanford Maternal & Child Health Research Institute (MCHRI), and California Institute for Regenerative Medicine. This work is supported by National Science Foundation CAREER award (Award #2046650), National Cancer Institute (Grant # 1U01DK127405, 1R01CA266470-01A1), and the Stanford MCHRI through the Uytengsu-Hamilton 22q11 Neuropsychiatry Research Award Program. L.S.Q. is a Chan Zuckerberg Biohub investigator.

AUTHOR CONTRIBUTIONS

P.B.F. and L.S.Q. conceived the idea. P.B.F., M.C., L.S.Q. planned the *in vitro* experiments. P.B.F., M.C., L.S.Q. planned the *in vivo* experiments. P.B.F. designed plasmids. P.B.F., D.R., X.C. cloned plasmids. P.B.F., M.C., X.C. performed cell culture experiments. H.W. performed confocal microscopy imaging experiments and analyzed imaging data. P.B.F. designed the DNA origami and biotin dendrimers. J.G. performed chemical synthesis of a biotin dendrimer compound. P.B.F., M.C., and L.S.Q. analyzed the experimental data. P.B.F., M.C., and L.S.Q wrote the manuscript. L.S.Q secured funding. All authors read and commented on the manuscript.

DECLARATION OF INTERESTS

The authors have filed provisional patents via Stanford University related to this work (PCT/US2022/079889). L.S.Q. is a founder of Epic Bio and a scientific advisor of Laboratory of Genomics Research and Kytopen. P.B.F and M.C are founders of Enoda Cellworks, Inc.

REFERENCES

1. L. Chen, D. B. Flies, Molecular mechanisms of T cell co-stimulation and co-inhibition. *Nat. Rev. Immunol.* **13**, 227 (2013).
2. A. Schnell, L. Bod, A. Madi, V. K. Kuchroo, The yin and yang of co-inhibitory receptors: toward anti-tumor immunity without autoimmunity. *Cell Res.* **30**, 285 (2020).
3. A. D. Waldman, J. M. Fritz, M. J. Lenardo, A guide to cancer immunotherapy: from T cell basic science to clinical practice. *Nat. Rev. Immunol.* **20**, 651 (2020).
4. M. A. Fischbach, J. A. Bluestone, W. A. Lim, Cell-based therapeutics: The next pillar of medicine. *Sci. Transl. Med.* **5**, 1 (2013).
5. W. A. Lim, The emerging era of cell engineering: Harnessing the modularity of cells to program complex biological function. *Science*. **378**, 848 (2022).
6. C. H. June, M. Sadelain, Chimeric Antigen Receptor Therapy. *new Engl. J. Med. Rev.* **379**, 64 (2018).
7. A. Alnefaie, S. Albogami, Y. Asiri, T. Ahmad, S. S. Alotaibi, M. M. Al-Sanea, H. Althobaiti, Chimeric Antigen Receptor T-Cells: An Overview of Concepts, Applications, Limitations, and Proposed Solutions. *Front. Bioeng. Biotechnol.* **10**, 1 (2022).
8. S. S. Neelapu, F. L. Locke, N. L. Bartlett, L. J. Lekakis, D. B. Miklos, C. A. Jacobson, I. Braunschweig, O. O. Oluwole, T. Siddiqi, Y. Lin, J. M. Timmerman, P. J. Stiff, J. W. Friedberg, I. W. Flinn, A. Goy, B. T. Hill, M. R. Smith, A. Deol, U. Farooq, P. McSweeney, J. Munoz, I. Avivi, J. E. Castro, J. R. Westin, J. C. Chavez, A. Ghobadi, K. V. Komanduri, R. Levy, E. D. Jacobsen, T. E. Witzig, P. Reagan, A. Bot, J. Rossi, L. Navale, Y. Jiang, J. Aycock, M. Elias, D. Chang, J. Wiezorek, W. Y. Go, Axicabtagene Ciloleucel CAR T-Cell Therapy in Refractory Large B-Cell Lymphoma. *N. Engl. J. Med.* **377**, 2531 (2017).
9. S. L. Maude, T. W. Laetsch, J. Buechner, S. Rives, M. Boyer, H. Bittencourt, P. Bader, M. R. Verneris, H. E. Stefanski, G. D. Myers, M. Qayed, B. De Moerloose, H. Hiramatsu, K. Schlis, K. L. Davis, P. L. Martin, E. R. Nemecek, G. A. Yanik, C. Peters, A. Baruchel, N. Boissel, F. Mechinaud, A. Balduzzi, J. Krueger, C. H. June, B. L. Levine, P. Wood, T. Taran, M. Leung, K. T. Mueller, Y. Zhang, K. Sen, D. Lebwohl, M. A. Pulsipher, S. A. Grupp, Tisagenlecleucel in Children and Young Adults with B-Cell Lymphoblastic Leukemia. *N. Engl. J. Med.* **378**, 439 (2018).
10. M. Wang, J. Munoz, A. Goy, F. L. Locke, C. A. Jacobson, B. T. Hill, J. M. Timmerman, H. Holmes, S. Jaglowski, I. W. Flinn, P. A. McSweeney, D. B. Miklos, J. M. Pagel, M.-J. Kersten, N. Milpied, H. Fung, M. S. Topp, R. Houot, A. Beitinjaneh, W. Peng, L. Zheng, J. M. Rossi, R. K. Jain, A. V. Rao, P. M. Reagan, KTE-X19 CAR T-Cell Therapy in Relapsed or Refractory Mantle-Cell Lymphoma. *N. Engl. J. Med.* **382**, 1331 (2020).
11. J. S. Abramson, M. L. Palomba, L. I. Gordon, M. A. Lunning, M. Wang, J. Arnason, A. Mehta, E. Purev, D. G. Maloney, C. Andreadis, A. Sehgal, S. R. Solomon, N. Ghosh, T. M. Albertson, J. Garcia, A. Kostic, M. Mallaney, K. Ogasawara, K. Newhall, Y. Kim, D. Li, T. Siddiqi, Lisocabtagene maraleucel for patients with relapsed or refractory large B-cell lymphomas (TRANSCEND NHL 001): a multicentre seamless design study. *Lancet*. **396**, 839 (2020).
12. A. D. Fesnak, C. H. June, B. L. Levine, Engineered T cells: The promise and challenges of cancer immunotherapy. *Nat. Rev. Cancer*. **16**, 566 (2016).
13. N. N. Shah, T. J. Fry, Mechanisms of resistance to CAR T cell therapy. *Nat. Rev. Clin. Oncol.* **16**, 372 (2019).
14. A. Schmidts, M. V. Maus, Making CAR T Cells a Solid Option for Solid Tumors. *Front. Immunol.* **9**, 2593 (2018).
15. L. Yan, B. Liu, Critical factors in chimeric antigen receptor-modified T-cell (CAR-T) therapy for solid tumors. *Onco. Targets. Ther.* **12**, 193 (2018).
16. M. Castellarin, K. Watanabe, C. H. June, C. C. Kloss, A. D. Posey, Driving cars to the clinic for solid tumors. *Gene Ther.* **25**, 165 (2018).
17. H. G. Caruso, L. V. Hurton, A. Najjar, D. Rushworth, S. Ang, S. Olivares, T. Mi, K. Switzer, H. Singh, H. Huls, D. A. Lee, A. B. Heimberger, R. E. Champlin, L. J. N. Cooper, Tuning sensitivity of CAR to EGFR density limits recognition of normal tissue while maintaining potent antitumor activity. *Cancer Res.* **75**, 3505 (2015).
18. K. Watanabe, S. Terakura, A. C. Martens, T. van Meerten, S. Uchiyama, M. Imai, R. Sakemura, T. Goto, R. Hanajiri, N. Imahashi, K. Shimada, A. Tomita, H. Kiyoi, T. Nishida, T. Naoe, M. Murata, Target Antigen Density Governs the Efficacy of Anti–CD20-CD28-CD3 ζ Chimeric Antigen Receptor–Modified Effector CD8 + T Cells. *J. Immunol.* **194**, 911 (2015).
19. A. J. Walker, R. G. Majzner, L. Zhang, K. Wanhainen, A. H. Long, S. M. Nguyen, P. Lopomo, M. Vigny, T. J. Fry, R. J. Orentas, C. L. Mackall, Tumor Antigen and Receptor Densities Regulate Efficacy of a Chimeric Antigen Receptor Targeting Anaplastic Lymphoma Kinase. *Mol. Ther.* **25**, 2189 (2017).
20. M. Ruella, M. V. Maus, Catch me if you can: Leukemia Escape after CD19-Directed T Cell Immunotherapies. *Comput. Struct. Biotechnol. J.* **14**, 357 (2016).
21. K. Watanabe, S. Kuramitsu, A. D. Posey, C. H. June, Expanding the Therapeutic Window for CAR T

Cell Therapy in Solid Tumors: The Knowns and Unknowns of CAR T Cell Biology. *Front. Immunol.* **9**, 2486 (2018).
22. R. G. Majzner, S. P. Rietberg, E. Sotillo, R. Dong, V. T. Vachharajani, L. Labanieh, J. H. Myklebust, M. Kadapakkam, E. W. Weber, A. M. Tousley, R. M. Richards, S. Heitzeneder, S. M. Nguyen, V. Wiebking, J. Theruvath, R. C. Lynn, P. Xu, A. R. Dunn, R. D. Vale, C. L. Mackall, Tuning the Antigen Density Requirement for CAR T Cell Activity. *Cancer Discov.* **10**, 702 (2020).
23. V. S. Sheth, J. Gauthier, Taming the beast: CRS and ICANS after CAR T-cell therapy for ALL. *Bone Marrow Transplant.* **56**, 552 (2021).
24. A. Schmidts, M. Wehrli, M. V. Maus, Toward Better Understanding and Management of CAR-T Cell-Associated Toxicity. *Annu. Rev. Med.* **72**, 365 (2021).
25. A. Hyrenius-Wittsten, K. T. Roybal, Paving New Roads for CARs. *Trends in Cancer*. **5** (2019), p. 583.
26. A. H. Courtney, W. L. Lo, A. Weiss, TCR Signaling: Mechanisms of Initiation and Propagation. *Trends Biochem. Sci.* **43**, 108 (2018).
27. R. T. Abraham, A. Weiss, Jurkat T cells and development of the T-cell receptor signalling paradigm. *Nat. Rev. Immunol.* **4** (2004), p. 301.
28. J. J. Boniface, J. D. Rabinowitz, C. W. Lfing, J. Hampl, Z. Reich, J. D. Altman, R. M. Kantor, C. Beeson, H. M. McConnell, M. M. Davis, Initiation of Signal Transduction through the T Cell Receptor Requires the Multivalent Engagement of Peptide/MHC Ligands. *Immunity*. **9**, 459 (1998).
29. J. R. Cochran, T. O. Cameron, J. D. Stone, J. B. Lubetsky, L. J. Stern, Receptor Proximity, Not Intermolecular Orientation, Is Critical tor Triggering T-cell Activation. *J. Biol. Chem.* **276**, 28068 (2001).
30. T. Yokosuka, K. Sakata-Sogawa, W. Kobayashi, M. Hiroshima, A. Hashimoto-Tane, M. Tokunaga, M. L. Dustin, T. Saito, Newly generated T cell receptor microclusters initiate and sustain T cell activation by recruitment of Zap70 and SLP-76. *Nat. Immunol.* **6**, 1253 (2005).
31. S. V. Pageon, T. Tabarin, Y. Yamamoto, Y. Ma, J. S. Bridgeman, A. Cohnen, C. Benzing, Y. Gao, M. D. Crowther, K. Tungatt, G. Dolton, A. K. Sewell, D. A. Price, O. Acuto, R. G. Parton, J. J. Gooding, J. Rossy, J. Rossjohn, K. Gaus, Functional role of T-cell receptor nanoclusters in signal initiation and antigen discrimination. *Proc. Natl. Acad. Sci. U. S. A.* **113**, E5454 (2016).
32. X. Su, J. A. Ditlev, E. Hui, W. Xing, S. Banjade, J. Okrut, D. S. King, J. Taunton, M. K. Rosen, R. D. Vale, Phase separation of signaling molecules promotes T cell receptor signal transduction. *Science*. **352**, 595 (2016).
33. H. Cai, J. Muller, D. Depoil, V. Mayya, M. P. Sheetz, M. L. Dustin, S. J. Wind, Full control of ligand positioning reveals spatial thresholds for T cell receptor triggering. *Nat. Nanotechnol.* **13**, 610 (2018).
34. A. K. Chakraborty, A. Weiss, Insights into the initiation of TCR signaling. *Nat. Immunol.* **15**, 798 (2014).
35. A. Hashimoto-Tane, T. Saito, Dynamic regulation of TCR-microclusters and the microsynapse for T cell activation. *Front. Immunol.* **7**, 1 (2016).
36. M. J. Taylor, K. Husain, Z. J. Gartner, S. Mayor, R. D. Vale, A DNA-Based T Cell Receptor Reveals a Role for Receptor Clustering in Ligand Discrimination. *Cell*. **169**, 108 (2017).
37. J. Goyette, D. J. Nieves, Y. Ma, K. Gaus, How does T cell receptor clustering impact on signal transduction? *J. Cell Sci.* **132**, jcs226423 (2019).
38. M. Sadelain, R. Brentjens, I. Rivière, The basic principles of chimeric antigen receptor design. *Cancer Discov.* **3**, 388 (2013).
39. A. J. Davenport, R. S. Cross, K. A. Watson, Y. Liao, W. Shi, H. M. Prince, P. A. Beavis, J. A. Trapani, M. H. Kershaw, D. S. Ritchie, P. K. Darcy, P. J. Neeson, M. R. Jenkins, Chimeric antigen receptor T cells form nonclassical and potent immune synapses driving rapid cytotoxicity. *Proc. Natl. Acad. Sci. U. S. A.* **115**, E2068 (2018).
40. W. Xiong, Y. Chen, X. Kang, Z. Chen, P. Zheng, Y.-H. Hsu, J. H. Jang, L. Qin, H. Liu, G. Dotti, D. Liu, Immunological Synapse Predicts Effectiveness of Chimeric Antigen Receptor Cells. *Mol. Ther.* **26**, 963 (2018).
41. D. Liu, S. Badeti, G. Dotti, J. G. Jiang, H. Wang, J. Dermody, P. Soteropoulos, D. Streck, R. B. Birge, C. Liu, The Role of Immunological Synapse in Predicting the Efficacy of Chimeric Antigen Receptor (CAR) Immunotherapy. *Cell Commun. Signal.* **18**, 1 (2020).
42. D. M. Spencer, T. J. Wandless, S. L. Schreiber, G. R. Crabtree, Controlling Signal Transduction with Ligands. *Science*. **262**, 1019 (1993).
43. Y. Ma, Y. J. Lim, A. Benda, J. Lou, J. Goyette, K. Gaus, Clustering of the ζ-chain can initiate t cell receptor signaling. *Int. J. Mol. Sci.* **21**, 1 (2020).
44. Y. Wang, Y. Gao, C. Niu, B. Wang, S. Zhao, G. Roex, J. Qian, J. Qie, L. Chen, C. Yi, S. Anguille, J. Liu, F. Luo, Y. Chu, Chimeric antigen receptor clustering via cysteines enhances T-cell efficacy against tumor. *Cancer Immunol. Immunother.* **71**, 2801 (2022).
45. K. H. Lim, H. Huang, A. Pralle, S. Park, Stable, high-affinity streptavidin monomer for protein labeling and monovalent biotin detection. *Biotechnol. Bioeng.* **110**, 57 (2013).
46. M. Słabicki, H. Yoon, J. Koeppel, L. Nitsch, S. S. Roy Burman, C. Di Genua, K. A. Donovan, A. S. Sperling, M. Hunkeler, J. M. Tsai, R. Sharma, A. Guirguis, C. Zou, P. Chudasama, J. A. Gasser, P. G. Miller, C. Scholl, S. Fröhling, R. P. Nowak, E. S. Fischer, B. L. Ebert, Small-molecule-induced

polymerization triggers degradation of BCL6. *Nature*. **588**, 164 (2020).
47. A. H. Long, W. M. Haso, J. F. Shern, K. M. Wanhainen, M. Murgai, M. Ingaramo, J. P. Smith, A. J. Walker, M. E. Kohler, V. R. Venkateshwara, R. N. Kaplan, G. H. Patterson, T. J. Fry, R. J. Orentas, C. L. Mackall, 4-1BB costimulation ameliorates T cell exhaustion induced by tonic signaling of chimeric antigen receptors. *Nat. Med.* **21**, 581 (2015).
48. R. C. Lynn, E. W. Weber, E. Sotillo, D. Gennert, P. Xu, Z. Good, H. Anbunathan, J. Lattin, R. Jones, V. Tieu, S. Nagaraja, J. Granja, C. F. A. de Bourcy, R. Majzner, A. T. Satpathy, S. R. Quake, M. Monje, H. Y. Chang, C. L. Mackall, c-Jun overexpression in CAR T cells induces exhaustion resistance. *Nature*. **576**, 293 (2019).
49. R. Sakemura, S. Terakura, K. Watanabe, J. Julamanee, E. Takagi, K. Miyao, D. Koyama, T. Goto, R. Hanajiri, T. Nishida, M. Murata, H. Kiyoi, A Tet-On Inducible system for controlling CD19-Chimeric antigen receptor expression upon drug administration. *Cancer Immunol. Res.* **4**, 658 (2016).
50. E. W. Weber, K. R. Parker, E. Sotillo, R. C. Lynn, H. Anbunathan, J. Lattin, Z. Good, J. A. Belk, B. Daniel, D. Klysz, M. Malipatlolla, P. Xu, M. Bashti, S. Heitzeneder, L. Labanieh, P. Vandris, R. G. Majzner, Y. Qi, K. Sandor, L. Chen, S. Prabhu, A. J. Gentles, T. J. Wandless, A. T. Satpathy, H. Y. Chang, C. L. Mackall, Transient rest restores functionality in exhausted CAR-T cells through epigenetic remodeling. *Science*. **372**, eaba1786 (2021).
51. A. C. Sahillioglu, M. Toebes, G. Apriamashvili, R. Gomez, T. N. Schumacher, Crash-it switch enables reversible and dose-dependent control of tcr and car t-cell function. *Cancer Immunol. Res.* **9**, 999 (2021).
52. L. Labanieh, R. Majzner, D. Klysz, C. J. Fisher, E. Sotillo, J. Vilches-Moure, K. Pacheco, M. Malipatlolla, P. Xu, J. Hui, T. Murty, J. Theruvath, N. Mehta, S. A. Yamada-Hunter, E. Weber, S. Heitzeneder, K. R. Parker, A. T. Satpathy, H. Y. Chang, M. Z. Lin, J. R. Cochran, C. L. Mackall, Enhanced safety and efficacy of protease-regulated CAR-T cell receptors. *Cell*, 1 (2022).
53. R. A. Hernandez-lopez, W. Yu, K. A. Cabral, O. A. Creasey, P. Lopez, Y. Tonai, A. De Guzman, A. Mäkelä, K. Saksela, Z. J. Gartner, W. A. Lim, T cell circuits that sense antigen density with an ultrasensitive threshold. *Science*. **371**, 1166 (2021).
54. C.-Y. Wu, K. T. Roybal, E. M. Puchner, J. Onuffer, W. A. Lim, Remote control of therapeutic T cells through a small molecule–gated chimeric receptor. *Science*. **350**, aab4077 (2015).
55. B. Salzer, C. M. Schueller, C. U. Zajc, T. Peters, M. A. Schoeber, B. Kovacic, M. C. Buri, E. Lobner, O. Dushek, J. B. Huppa, C. Obinger, E. M. Putz, W. Holter, M. W. Traxlmayr, M. Lehner, Engineering AvidCARs for combinatorial antigen recognition and reversible control of CAR function. *Nat. Commun.* **11**, 4166 (2020).
56. S. Carbonneau, S. Sharma, L. Peng, V. Rajan, D. Hainzl, M. Henault, C. Yang, J. Hale, J. Shulok, J. Tallarico, J. Porter, J. L. Brogdon, G. Dranoff, J. E. Bradner, M. Hild, C. P. Guimaraes, An IMiD-inducible degron provides reversible regulation for chimeric antigen receptor expression and activity. *Cell Chem. Biol.* **28**, 802 (2021).
57. M. Jan, I. Scarfò, R. C. Larson, A. Walker, A. Schmidts, A. A. Guirguis, J. A. Gasser, M. Słabicki, A. A. Bouffard, A. P. Castano, M. C. Kann, M. L. Cabral, A. Tepper, D. E. Grinshpun, A. S. Sperling, T. Kyung, Q. L. Sievers, M. E. Birnbaum, M. V. Maus, B. L. Ebert, Reversible ON- And OFF-switch chimeric antigen receptors controlled by lenalidomide. *Sci. Transl. Med.* **13**, 1 (2021).
58. G. Liu, L. Yang, G. Chen, F. Xu, F. Yang, H. Yu, L. Li, X. Dong, J. Han, C. Cao, J. Qi, J. Su, X. Xu, X. Li, B. Li, A Review on Drug Delivery System for Tumor Therapy. *Front. Pharmacol.* **12**, 1 (2021).
59. C. L. Flugel, R. G. Majzner, G. Krenciute, G. Dotti, S. R. Riddell, D. L. Wagner, M. Abou-el-Enein, Overcoming on-target, off-tumour toxicity of CAR T cell therapy for solid tumours. *Nat. Rev. Clin. Oncol.* (2022).
60. C. C. Zebley, B. Youngblood, CAR T cells need a pitstop to win the race. *Cancer Cell*. **39**, 756 (2021).
61. N. Philipp, M. Kazerani, A. Nicholls, B. Vick, J. Wulf, T. Straub, M. Scheurer, A. Muth, G. Hänel, D. Nixdorf, M. Sponheimer, M. Ohlmeyer, S. M. Lacher, B. Brauchle, A. Marcinek, L. Rohrbacher, A. Leutbecher, K. Rejeski, O. Weigert, M. von Bergwelt-Baildon, S. Theurich, R. Kischel, I. Jeremias, V. Bücklein, M. Subklewe, T-cell exhaustion induced by continuous bispecific molecule exposure is ameliorated by treatment-free intervals. *Blood*. **140**, 1104 (2022).